

CIRCULATION COPY
SUBJECT TO RECALL
IN TWO WEEKS

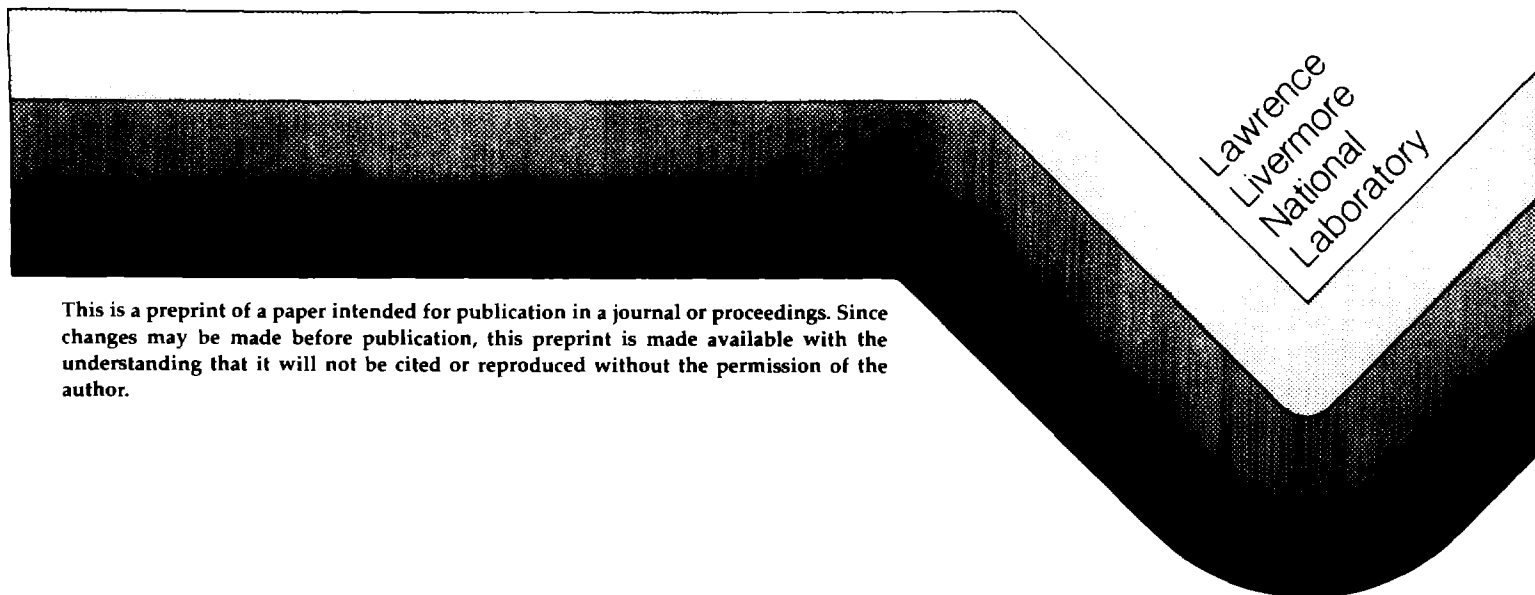
UCRL-92608
PREPRINT

Collision Broadened Resonance Localization
in Tokamaks Excited with ICRF Waves

G. D. Kerbel and M. G. McCoy

This paper was prepared for submittal to the
3rd European Workshop on Problems in the
Numerical Modeling of Plasmas (NUMOP 85),
Varenna, Italy, September 10-13, 1985

August 1985



This is a preprint of a paper intended for publication in a journal or proceedings. Since changes may be made before publication, this preprint is made available with the understanding that it will not be cited or reproduced without the permission of the author.

DISCLAIMER

This document was prepared as an account of work sponsored by an agency of the United States Government. Neither the United States Government nor the University of California nor any of their employees, makes any warranty, express or implied, or assumes any legal liability or responsibility for the accuracy, completeness, or usefulness of any information, apparatus, product, or process disclosed, or represents that its use would not infringe privately owned rights. Reference herein to any specific commercial products, process, or service by trade name, trademark, manufacturer, or otherwise, does not necessarily constitute or imply its endorsement, recommendation, or favoring by the United States Government or the University of California. The views and opinions of authors expressed herein do not necessarily state or reflect those of the United States Government or the University of California, and shall not be used for advertising or product endorsement purposes.

Collision Broadened Resonance Localization in Tokamaks Excited with ICRF Waves *

G. D. Kerbel and M. G. McCoy

National Magnetic Fusion Energy Computer Center
Lawrence Livermore National Laboratory

Advanced wave models used to evaluate ICRH in tokamaks typically use warm plasma theory and allow inhomogeneity in one dimension. The majority of these calculations neglect the fact that gyro-centers experience the inhomogeneity via their motion parallel to the magnetic field. The non-local effects of rotational transform and toroidicity can play a significant role in both the propagation and the absorption physics. In strongly driven systems, wave damping can distort the particle distribution function supporting the wave and this produces changes in the absorption. The most common approach is to use Maxwellian absorption rates calculated in uniform magnetic field. We have developed a bounce-averaged Fokker-Planck quasilinear computational model which evolves the population of particles on more realistic orbits. Each wave-particle resonance has its own specific interaction amplitude within any given volume element. These data need only be generated once, and appropriately stored for efficient retrieval. The wave-particle resonant interaction then serves as a mechanism by which the diffusion of particle populations can proceed among neighboring orbits. Collisions affect the absorption of RF energy by two quite distinct processes: In addition to the usual relaxation towards the Maxwellian distribution creating velocity gradients which drive quasilinear diffusion, collisions also affect the wave-particle resonance through the mechanism of gyro-phase diffusion.

The local specific spectral energy absorption rate is directly calculable once the orbit geometry and populations are determined. The code is constructed in such fashion as to accomodate wave propagation models which provide the wave spectral energy density on a poloidal cross-section. Information provided by the calculation includes the local absorption properties of the medium which can then be exploited to evolve the wave field.

RF Power Absorption: Collisionless Theory

The RF power absorbed on a flux surface per unit toroidal extent by resonant particles can be represented in terms of the quasilinear component of the Fokker-Planck operator:

$$P_{RF} = \int d^3v_0 \frac{1}{2} m v_0^2 \frac{\partial \lambda \mathcal{F}_0}{\partial t} = - \int d^3v_0 \frac{1}{2} m v_0^2 \nabla_{\mathbf{v}_0} \cdot \hat{\Gamma}_{0q}.$$

* Work performed under the auspices of the U.S.D.O.E. by LLNL under contract No. W-7405-ENG-48.

where $\lambda = v_0 \cos \theta_0 \tau_B$, τ_B is the bounce period, and all quantities are represented in the constants-of-motion (velocity) space (v_0, θ_0) . After an integration by parts, the RF power absorbed can be cast in the form

$$P_{RF} = -2\pi \int dv_0 \int d\theta_0 m v_0 \sin \theta_0 B_{0_{q_l}} \hat{\Delta}_0 \mathcal{F}_0 \quad (1)$$

where the differential operator $\hat{\Delta}_0$ is given by

$$\hat{\Delta}_0 = \frac{\partial}{\partial v_0} + \frac{m\Omega_0/\omega - \sin^2 \theta_0}{v_0 \sin \theta_0 \cos \theta_0} \frac{\partial}{\partial \theta_0},$$

the bounce-averaged quasilinear coefficient $B_{0_{q_l}}$ can be expressed in the form

$$B_{0_{q_l}} = -\lambda \frac{q^2}{4m^2} \sum_n I_n.$$

and the trajectory integral I_n appearing in the definition of $B_{0_{q_l}}$ can be represented as

$$I_n = \oint d\tau \left(\Pi_n(\tau) e^{i\Psi(\tau)} \right)^* \frac{\Upsilon}{\tau_B} \int_{\tau-\tau_B}^{\tau} d\tau' \left(\Pi_n(\tau') e^{i\Psi(\tau')} \right) + cc. \quad (2)$$

The quantity $\Pi_n(\tau) = v \sin \theta \mathbf{E}_k \cdot \Theta_n$ denotes the amplitude of the n^{th} gyro-harmonic wave-particle interaction along the unperturbed gyro-center orbit.¹ It can be viewed as a slowly varying quantity in the sense that its time variation scales with the bounce time, ie. $\dot{\Pi}/\Pi \sim \omega_B \ll \Omega$. The eikonal Ψ given by

$$\Psi(n, t) = \int_0^t d\tau (n\Omega' + k'_{\parallel} v'_{\parallel} - \omega) = \int_0^t d\tau \nu(n, \tau) \quad (3)$$

represents the advance of the interaction phase, ν , along a given gyro-center trajectory. In large gyration frequency theory, $\Psi \sim \Omega\tau_B \gg 1$, so that Ψ is viewed as rapidly varying, and $\Omega\tau_B$ serves as the large parameter in the asymptotic analysis. The quantity referred to as Υ , which accounts for multiple-bounce coherence effects, the stacked *echoes* of prior resonances, is generally quite close to unity due to gyro-phase diffusion. This aspect of the theory will be discussed in more detail presently. First, however, let us examine the collisionless case neglecting gyro-phase diffusion.

The trajectory integrals in (2) may be approximated asymptotically ($\Omega\tau_B \rightarrow \infty$) by the method of stationary phase due to the rapid variation with τ of Ψ . The eikonal Ψ is expanded about the point where $d\Psi/dt$ vanishes (elsewhere the rapid oscillations provide cancelling contributions to the integrand). By (3), this implies

$$\frac{d\Psi}{dt} = \frac{d}{dt} \int_0^t d\tau \nu(n, \tau) = \nu(n, t) = 0. \quad (4)$$

the condition of wave-particle resonance. Near the stationary phase points we expand the (rapidly oscillating phase) factor Ψ as:

$$\Psi = \Psi_R + \nu \Delta\tau + \dot{\nu} \frac{\Delta\tau^2}{2!} + \ddot{\nu} \frac{\Delta\tau^3}{3!} + \dots, \quad (5)$$

$\Delta\tau$ being measured from the stationary phase point, $\nu(\tau_i) = 0$ (ie. $\Delta\tau = \tau - \tau_i$). Forming the trajectory integral in a neighborhood of τ_i , we can write

$$|\tau_{ci}| = \left| \int_{-D\tau}^{+D\tau} d\Delta\tau \exp \left[i \left(\Psi_R + \nu \Delta\tau + \dot{\nu} \frac{\Delta\tau^2}{2!} + \ddot{\nu} \frac{\Delta\tau^3}{3!} \right) \right] \right|. \quad (6)$$

Passing to the limit $D\tau \rightarrow \infty$, (6) becomes

$$\lim_{D\tau \rightarrow \infty} |\tau_{ci}| = \left| e^{i\Psi_R(\tau_i)} \int_{-\infty}^{+\infty} d\Delta\tau \exp \left[i \dot{\nu} \frac{\Delta\tau^2}{2!} \right] \right| = \left| e^{i(\Psi_R + \pi/4)} \sqrt{\frac{2\pi}{\dot{\nu}}} \right|. \quad (7)$$

At points for which $dB/d\tau = 0$ coincidentally with resonances, not only is $\nu = 0$, but also $\dot{\nu} = 0$. The expansion of Ψ about these points must retain the term in $\ddot{\nu}$; the resultant integral has the form of an Airy integral:

$$|\tau_c| = \left| e^{i\Psi_R} \int_{-\infty}^{+\infty} d\Delta\tau \exp \left[i \left(\nu \Delta\tau + \ddot{\nu} \frac{\Delta\tau^3}{3!} \right) \right] \right| = \left| 2\pi \sqrt[3]{\frac{2}{\ddot{\nu}}} Ai \left(\nu \sqrt[3]{\frac{2}{\ddot{\nu}}} \right) \right| \quad (8)$$

For $k_{\parallel} \neq 0$, the coalescence of two resonances can occur where $dB/d\tau \neq 0$ which adds some new twists to the calculation. This subject is treated in detail in Killeen, et al.¹

Associated with the timelike quantity τ_c through the evaluation of Ψ at the point of stationary phase is a certain phase factor (7). It is the advance of this phase between subsequent resonances which determines the single-bounce coherence of sequential wave-particle interactions. Orbit resonances too close to sense significant gyro-phase diffusion can interfere constructively or destructively through the action of the relative interaction phase separating them. Details of the calculation pertaining to this phenomenon are discussed in Kerbel and McCoy².

For the simplest case of isolated resonances ($\dot{\nu} \neq 0$), we can evaluate the (inner) phase integral in (2) to find

$$I_n = \oint d\tau \left(\Pi_n(\tau) e^{i\Psi(\tau)} \right)^* \frac{\Upsilon}{\tau_B} \Pi_n(\tau_R) |\tau_c| \times \begin{cases} e^{i(\Psi_R + \pi/4)} \left(1 + e^{-2i(\Psi_R + \pi/4)} \right) & \text{for } \tau \in \mathcal{C}^\dagger \\ e^{i(\Psi_R^\dagger + \pi/4)} \left(1 + e^{-2i(\Psi_R^\dagger + \pi/4)} \right) & \text{for } \tau \in \mathcal{C} \end{cases} + cc. \quad (9)$$

The division of a trapped gyro-center trajectory into single-cycle complements \mathcal{C} and \mathcal{C}^\dagger is shown in Figure 1. Completing the outer integral there results

$$I_n = 4\Pi_n^2(\tau_R) |\tau_c|^2 \Upsilon \left\{ \alpha(1 - \sin 2\Psi_R^\dagger) + (1 - \alpha)(1 - \sin 2\Psi_R) \right\}, \quad (10)$$

where we have defined

$$2\Psi_R = \int_C d\tau \nu(\tau); \quad 2\Psi_R^\dagger = \int_{C^\dagger} d\tau \nu(\tau); \quad \text{and} \quad \alpha = \int_C d\tau / \tau_B.$$

The single-bounce coherence effects appear through the presence of the trigonometric terms in I_n whose arguments are just the advance of the interaction phase between subsequent resonances (over the two complementary paths comprising a single-bounce cycle).

Collisional Resonant Diffusion

The model just described centers on the mechanism of magnetic decorrelation. Though a charged particle must be in resonance to interact strongly with the exciting RF fields, it is not the case that the magnetic correlation time $|\tau_c|$ is the most rational measure of the strength of the interaction in all cases. In some cases of interest, finite bandwidth wave spectra give rise to shorter wave-particle correlation times. Moreover, including collisional effects can significantly alter the calculation of the effective correlation times-especially in cases for which the magnetic field is nearly uniform-through the mechanism of gyro-phase diffusion. Better realism, as well as computational convenience and completeness, are among the incentives to generalize the unperturbed collisionless orbits to include the effects of collisions on an *a priori* basis.

The effect can be most clearly understood by considering the uniform magnetic field case. In collisionless theory, those ions whose gyro-centers lie on resonant orbits remain in resonance for all time; ions on orbits nearby in the constants-of-motion space realize no resonant diffusion whatever. The resonant diffusion thus has measure (one) support in the constants-of-motion space and has the mathematical form of a generalized function or distribution. This aspect of the theory allows the analytic evaluation of certain quantities of interest, in particular, the power absorption. However, in contradistinction to the analytic theory, this (idealized) structure becomes increasingly difficult to detect with a finite analysis numerical scheme as the magnetic field inhomogeneity vanishes. For such cases, the (collisionless) magnetic correlation time is either longer than the gyro-phase diffusion time or undefined. Collisions decorrelate the wave-particle resonance and limit the energy exchange between the particle and the wave field. The presence of a large multiplicative factor of the pitchangle scattering rate in the gyro-phase diffusion is responsible for the importance of this effect even deeply within the (collisionless) banana regime.

The physical mechanism at work here is clear. Small angle coulomb collisions alter the trajectory of a particle which is in resonance with the wave field, causing the resonant exchange of energy between the field and the particle to slow, stop, or reverse. The inverse process can also occur: A particle not initially on a resonant trajectory can experience resonant interaction through the mediation of collisional processes.

In order to include the effects of collisions within this formalism, we introduce a gyro-phase diffusion kernel $\Phi(\delta\phi, \Delta\tau) = \exp(i\delta\phi) P(\delta\phi, \Delta\tau = \tau_1 - \tau_2)$ to describe the evolution during the time interval $\Delta\tau$ along a gyro-center trajectory of the probability distribution of cumulative random gyro-phase increments $\delta\phi$ due to pitchangle scattering. Our aim, once having

chosen a model for calculating Φ , will be to perform the ensemble average over increments $\delta\phi$ using the appropriate $\Delta\tau$, thus revealing the gyro-phase diffused analog to expression (10).

To this end we require that Φ have the following properties: (1) $\int d\delta\phi P = 1$, the kernel is normalized; (2) $\int d\delta\phi \delta\phi P = 0$, it is symmetric; and (3) $\int d\delta\phi \delta\phi^2 P = \langle \Delta\phi^2 \rangle (\Delta\tau) \sim \gamma(v_0, \theta_0) \nu_{ii} \Omega^2 \Delta\tau^3$, its dispersion solves Langevin equations for the cumulative diffusion of the gyro-phase angle due to pitch-angle scattering (see for example Cohen, et al.³). The function γ is of order unity and depends on particulars of the magnetic field geometry.

Applying the diffusion kernel to expression (2) and indicating the appropriate ensemble average we obtain

$$I_n = \int d\delta\phi \oint d\tau \left(\Pi_n(\tau) \Phi(\delta\phi, \Delta\tau) e^{i\Psi(\tau)} \right)^* \times \frac{\Upsilon}{\tau_B} \int d\delta\phi' \int_{\tau-\tau_B}^{\tau} d\tau' \Pi_n(\tau') \Phi(\delta\phi', \Delta\tau') e^{i\Psi(\tau')} + cc. \quad (11)$$

where $\Delta\tau = \tau_R - \tau$. A calculation similar to that leading to (9) results in its gyro-phase diffused counterpart

$$I_n = \int d\delta\phi \oint d\tau \left(\Pi_n(\tau) \Phi(\delta\phi, \Delta\tau) e^{i\Psi(\tau)} \right)^* \frac{\Upsilon}{\tau_B} \Pi_n(\tau_R) |\tau_c| \times \int d\delta\phi' \begin{cases} e^{i(\Psi_R + \pi/4)} \left(\Phi(\delta\phi', 0) + \Phi(\delta\phi', 2\tau_R) e^{-2i(\Psi_R + \pi/4)} \right) & \text{for } \tau \in \mathcal{C}^\dagger \\ e^{i(\Psi_R^\dagger + \pi/4)} \left(\Phi(\delta\phi', 0) + \Phi(\delta\phi', \tau_B - 2\tau_R) e^{-2i(\Psi_R^\dagger + \pi/4)} \right) & \text{for } \tau \in \mathcal{C} \end{cases} + cc. \quad (12)$$

Choosing a Gaussian model for Φ is convenient and adequate for our purposes:

$$\Phi = \frac{\exp[i\delta\phi - \delta\phi^2/2\langle\Delta\phi^2\rangle(\Delta\tau)]}{\sqrt{2\pi\langle\Delta\phi^2\rangle(\Delta\tau)}}$$

Completing the outer τ integral and performing the ensemble averages over $\delta\phi$ and $\delta\phi'$ we obtain

$$I_n = 2\Pi_n^2(\tau_R) |\tau_c|^2 \Upsilon \left\{ \alpha(1 + e^{-2D^\dagger} - 2e^{-D^\dagger} \sin 2\Psi_R^\dagger) + (1 - \alpha)(1 + e^{-2D} - 2e^{-D} \sin 2\Psi_R) \right\} \quad (13)$$

where $D = 2\langle\Delta\phi^2\rangle(2\tau_R)$ and $D^\dagger = 2\langle\Delta\phi^2\rangle(\tau_B - 2\tau_R)$. This result expresses the fact that collisions destroy the phase coherence between subsequent resonant wave-particle interactions through the cumulative diffusion of the gyro-phase. The factor Υ representing the gyro-phase diffused sum over prior bounces of result (13) can be written as

$$\Upsilon = \sum_{n=0}^{\infty} \cos n\Psi_x \exp[-2\langle\Delta\phi^2\rangle(n\tau_B)] = \sum_{n=0}^{\infty} \cos n\Psi_x \exp[-2\gamma\nu_{ii}\Omega^2\tau_B^3 n^3] \quad (14)$$

where Ψ_x is the total advance of the interaction phase ν over a bounce period.

In reality the wave-particle resonant interactions are not confined to the instants τ_R , but rather occur over an interval corresponding in duration roughly to $|\tau_c|$ about τ_R . For sufficiently long $|\tau_c|$, gyro-phase diffusion can generate incoherence during the time $|\tau_c|$, limiting the strength of the resonant interaction. This situation arises most notably for shallow magnetic wells, coalescent resonances, or nearly uniform magnetic field.

To model the intra-resonant effects of gyro-phase diffusion on $|\tau_c|$ implicit in (12-13), we have applied the diffusion kernel Φ in equation (6):

$$|\tau_{ci}| = \left| \int d\delta\phi \int_{-D\tau}^{+D\tau} d\Delta\tau \Phi(\delta\phi, \Delta\tau) \exp \left[i \left(\Psi_R + \nu\Delta\tau + \dot{\nu} \frac{\Delta\tau^2}{2!} + \ddot{\nu} \frac{\Delta\tau^3}{3!} \right) \right] \right|. \quad (15)$$

Inverting the order of integration over $\tau(\tau')$ and $\delta\phi(\delta\phi')$ and passing to the limit $D\tau \rightarrow \infty$ (15) becomes

$$\lim_{D\tau \rightarrow \infty} |\tau_{ci}| = \left| e^{i\Psi_R(\tau_i)} \int_{-\infty}^{+\infty} d\Delta\tau \exp \left[i\dot{\nu} \frac{\Delta\tau^2}{2!} - \gamma(v_0, \theta_0) \nu_{ii} \Omega^2 \Delta\tau^3 \right] \right|. \quad (16)$$

The limiting behavior of this integral as $\dot{\nu} \rightarrow 0$ is readily obtained as

$$\lim_{\dot{\nu} \rightarrow 0} |\tau_c| = \frac{(1/3)!}{\sqrt[3]{\gamma \nu_{ii} \Omega^2}}.$$

However, in actuality, the situation $\dot{\nu} \rightarrow 0$ represents the coalescence of two resonances as discussed with regard to (8). Following a procedure similar to that leading from (6-7) \mapsto (15-16) we obtain the corresponding gyro-phase diffused generalization of (8):

$$\begin{aligned} |\tau_c| &= \left| e^{i\Psi_R} \int_{-\infty}^{+\infty} d\Delta\tau \exp \left[i \left(\nu\Delta\tau + \ddot{\nu} \frac{\Delta\tau^3}{3!} \right) - \gamma(v_0, \theta_0) \nu_{ii} \Omega^2 \Delta\tau^3 \right] \right| \\ &= \left| 2\pi \sqrt[3]{\frac{2}{\ddot{\nu} + i 3! \gamma \nu_{ii} \Omega^2}} Ai \left(\nu \sqrt[3]{\frac{2}{\ddot{\nu} + i 3! \gamma \nu_{ii} \Omega^2}} \right) \right| \end{aligned} \quad (17)$$

The physical significance of this result is the existence of a boundary layer in the constants-of-motion space about the collisionless (undiffused) resonance whose width scales as $\sqrt[3]{\nu_{ii}}$. The effect is closely related to that reported by Auerbach⁴ in connection with Langmuir wave damping. He notes that in the collisionless limit the perturbed distribution in the boundary layer scales as $1/\sqrt[3]{\nu_{ii}}$ so that the damping rate is independent of collisionality. Collisionally broadened gyro-center orbits in the layer experience resonant interaction with the wave field and thus contribute to absorption. Since this boundary layer retains a calculable structure in the uniform field limit, our numerical scheme can be used to recover results accessible to analytic theory as well.

Resonance Localization

In order to determine the spacial (poloidal) variation of RF power absorption we introduce a numerical resonance broadening model which replaces the exponential in the integrand of (2)

by a resonance weighting function $w(\tau)$ and represent the phase integral in (2) mnemonically by

$$\int d\tau \Pi_n(\tau) e^{i\Psi(\tau)} \longmapsto \int d\tau \Pi_n |\tau_c| w(\tau) \quad (18)$$

where $|\tau_c|$ is identified through (7-8) or their collisional counterparts (16-17). The weighting function $w(\tau)$ is defined such that $\int d\tau w(\tau) = 1$, it is normalized; $\int d\tau \tau w(\tau) = \tau_R$, it is centered on the wave-particle resonance; and finally, $\int d\tau (\tau - \tau_R)^2 w(\tau) = |\tau_c|^2$, its width corresponds to the wave-particle correlation time. The unmodified application of the stationary phase method corresponds to a weighting function with point support, $w(\tau) = \delta(\tau - \tau_R)$. Figure 2 shows some aspects of the implementation of the weighting function technique. The parameter κ is adjustable; points τ_l correspond to poloidal angles θ_p on a fixed mesh; the integral $\int d\tau w$ is subdivided so as to provide the appropriate partial weights for each poloidal meshpoint, w_l . These partial weights are then stored dynamically in a packed array whose elements have the structure (l, w_l) . Since the w_l must all be smaller than 1, unpacking the array is trivial. Figure 3 shows the relationship between the approximant $w(\tau)$ and the interaction function in the vicinity of a turning point resonance.

This numerical technique is designed to provide computational convenience tempered by theoretical generalization. It is a physically motivated artifice which permits the wave damping calculated through the quasilinear model to be used concurrently with a wave propagation calculation; its design accomodates a wide variety of such propagation calculations, even those which presume a uniform magnetic field.

For the case of Tokamak geometry, we introduce the change of variables $w(\tau) \rightarrow W(\theta_p)$ and set

$$B_{0_{q_l}} = \bar{b}_0 \int d\theta_p W(\theta_p) \mathcal{E}_k(\theta_p).$$

The quantities \bar{b}_0 and W are functions of orbit invariants v_0, θ_0 as well as wave field parameters $\omega, k_{\parallel}, k_{\perp}$ and wave polarization at resonance. There is in general a certain group of gyro-center orbits each within its own range of resonant interaction at θ_p . The particles which populate these orbits all experience the same field spectral energy density \mathcal{E}_k at θ_p , though each with its own orbit dependent wave-particle coupling strength $W(\theta_p)$. It is the distribution of population over this orbit group which determines the absorption (or emission) at θ_p .

Figure 4 shows the phaseflow corresponding to the set of velocity space meshpoints chosen to represent the ion distribution \mathcal{F} . The abscissa corresponds to the poloidal angle, θ_p . The ordinate is the cosine of the pitchangle along a gyro-center trajectory. The orbits above the separatrix correspond to co-passing orbits, those below the separatrix correspond to counter-passing orbits, and the elliptical trajectories correspond to trapped orbits. Since kinetic energy is a constant of the unperturbed motion, these orbits are independent of v_0 . The vertical curves in Figure 4 represent the relation $\nu = 0$ in this space for a set of values v_0 . The solid curves are those for which $k_{\parallel} > 0$ and the dotted curves are those for which $k_{\parallel} < 0$. The intersections of the gyro-center trajectories and the curves $\nu = 0$ are the resonances corresponding to positions of stationary wave-particle interaction phase. For $k_{\parallel} = 0$, the vertical curves all collapse into a single vertical line passing through the common intersection of the curves. That intersection becomes the turning point or bounce resonance point. For $k_{\parallel} \neq 0$

the loci of points in the phase space at which wave-particle resonance occurs coincidentally with $\dot{\nu} = 0$, tangent resonance, is shown as the remaining curve in Figure 4. This curve, of course, also goes through the turning point resonance, since there is no parallel Doppler shift at that point. Figure 5 shows the interaction function and its variation with collisionality in the vicinity of a turning point resonance. Also shown is the corresponding vicinity in the gyro-center phase flow. Figure 6 shows the wave-particle interaction function and its variation with collisionality and magnetic field inhomogeneity (\vec{B}) in the vicinity of a field extremum resonance. As the magnetic field becomes more uniform, the resonance broadens to fill the envelope defined by the accumulation of gyro-phase incoherence due to collisions.

The differential power absorption can now be represented as the integral

$$\frac{dP_{RF}}{d\theta_p} = -2\pi \int dv_0 \int d\theta_0 m v_0 \sin \theta_0 \bar{b}_0 W \mathcal{E}_{\mathbf{k}} \hat{\Delta}_0 \mathcal{F}_0 \quad (19)$$

which is depicted in Figure 7. The depression in the power absorption near the fundamental resonance is a reflection of the fact that for moderate k_{\parallel} , only low energy particles experience vanishingly small doppler shift.

References

- ¹J. Killeen, G. D. Kerbel, M. G. McCoy, and A. A. Mirin, *Computational Methods for Kinetic Models of Magnetically Confined Plasmas*, Springer-Verlag, to be published.
- ²G. D. Kerbel and M. G. McCoy, *Kinetic Theory and Simulation of Multi-Species Plasmas in Tokamaks Excited With ICRF Waves*, UCRL-92062, LLNL, (1984); to be published Phys. Fluids (November, 1985).
- ³B. I. Cohen, R. H. Cohen, and T. D. Rognlien, Phys. Fluids, **26**, 808 (1983).
- ⁴S. P. Auerbach, Phys. Fluids, **20**, 1836 (1977).

Figure Captions

FIG. 1. **Trapped gyro-center trajectory single-cycle complements C and C^\dagger .** While on $C(C^\dagger)$ the incoherence associated with the most recent resonance pair occurred over path $C^\dagger(C)$.

FIG. 2. **Implementation of the weighting function technique.** The parameter κ is adjustable; points τ_l correspond to poloidal angles θ_p on a fixed mesh; the integral $\int d\tau w$ is subdivided so as to provide the appropriate partial weights for each poloidal meshpoint, w_l .

FIG. 3. **Relationship between $w(\tau)$ and the wave-particle interaction function.** The picture is drawn in the vicinity of turning point resonance

FIG. 4. **Phaseflow corresponding to the set of velocity space meshpoints chosen to represent the distribution \mathcal{F} .** The abscissa is the arclength along the magnetic field measured from the midplane normalized to the arclength from the midplane (minimum B) to the throat (maximum B). The ordinate is the cosine of the pitchangle along a gyrocenter trajectory. The orbits above the separatrix correspond to co-passing orbits, those below the separatrix correspond to counter-passing orbits, and the elliptical trajectories correspond to trapped orbits. Since kinetic energy is a constant of the motion, these orbits are independent of v_0 . The vertical curves represent the relation $\nu = \omega - k_{\parallel}v_{\parallel} - m\Omega = 0$ in this space for a set of values v_0 on the chosen velocity mesh. The solid curves are those for which $k_{\parallel} > 0$ and the dotted curves are those for which $k_{\parallel} < 0$. The intersections of the gyrocenter trajectories and the curves $\nu = 0$ are the resonances corresponding to positions of stationary wave-particle interaction phase. For $k_{\parallel} = 0$, the vertical curves all collapse into a single vertical line passing through the common intersection of the curves. That intersection corresponds to the turning point resonance. For $k_{\parallel} \neq 0$ the loci of points in the phase space at which wave-particle resonance occurs coincidentally with $\dot{\nu} = 0$, tangent resonance, is shown as the remaining curve. This curve, of course, also goes through the turning point resonance, since there is no parallel Doppler shift at that point.

FIG. 5. **The wave-particle interaction function (the acceleration in the particle frame) and its variation with collisionality in the vicinity of a turning point resonance.** Also shown is the corresponding gyro-center phase flow and resonance configuration

FIG. 6. **The wave-particle interaction function and its variation with collisionality and magnetic field inhomogeneity (\ddot{B}) in the vicinity of a field extremum resonance.** As the magnetic field becomes more uniform, the resonance broadens to fill the envelope defined by the collisional erosion of gyro-phase coherence.

FIG. 7. **Differential power absorption as a function of poloidal angle.** The depression in the power absorption near the fundamental resonance is a reflection of the fact that for moderate k_{\parallel} , only low energy particles experience vanishingly small doppler shift.

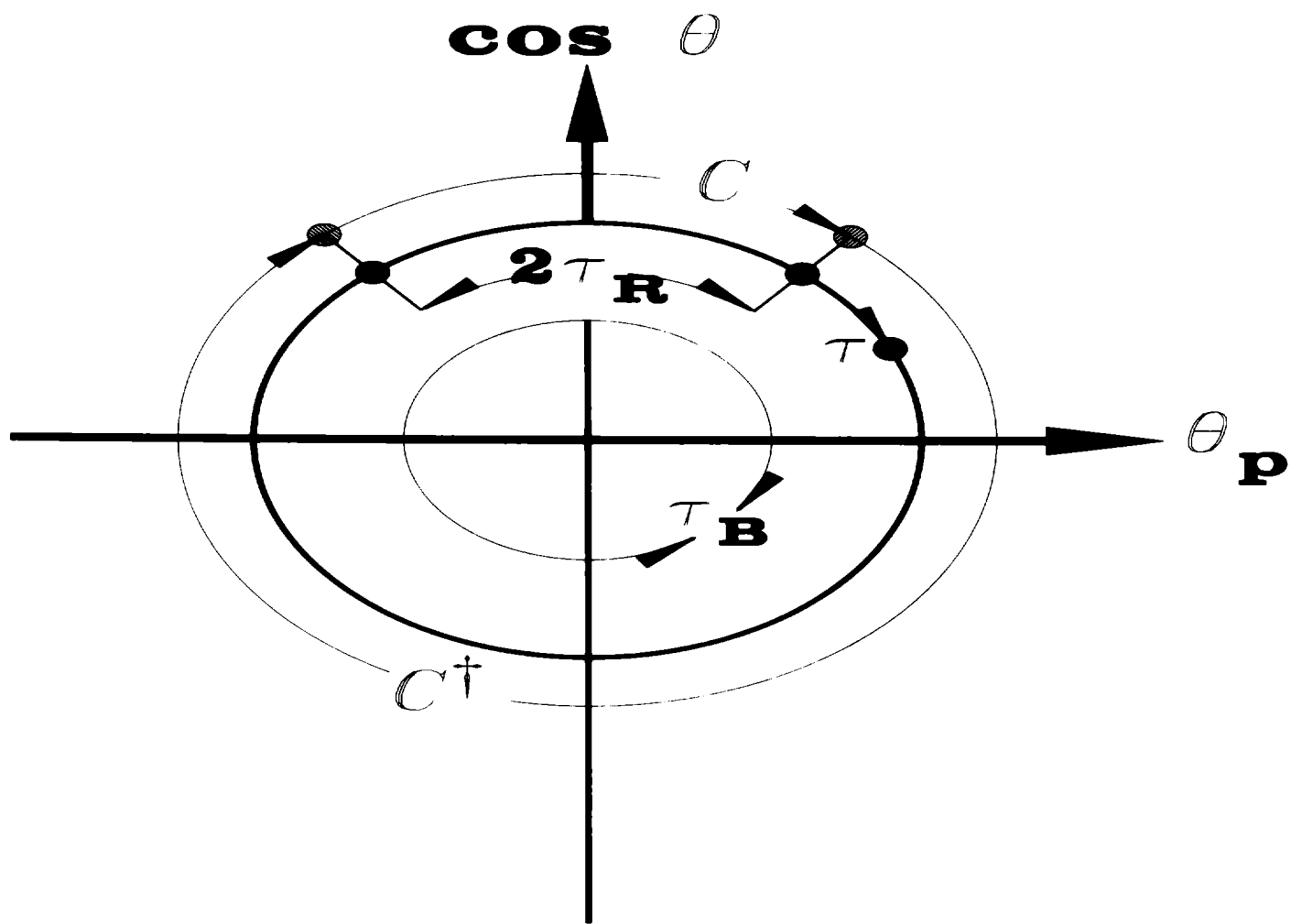


Figure 1

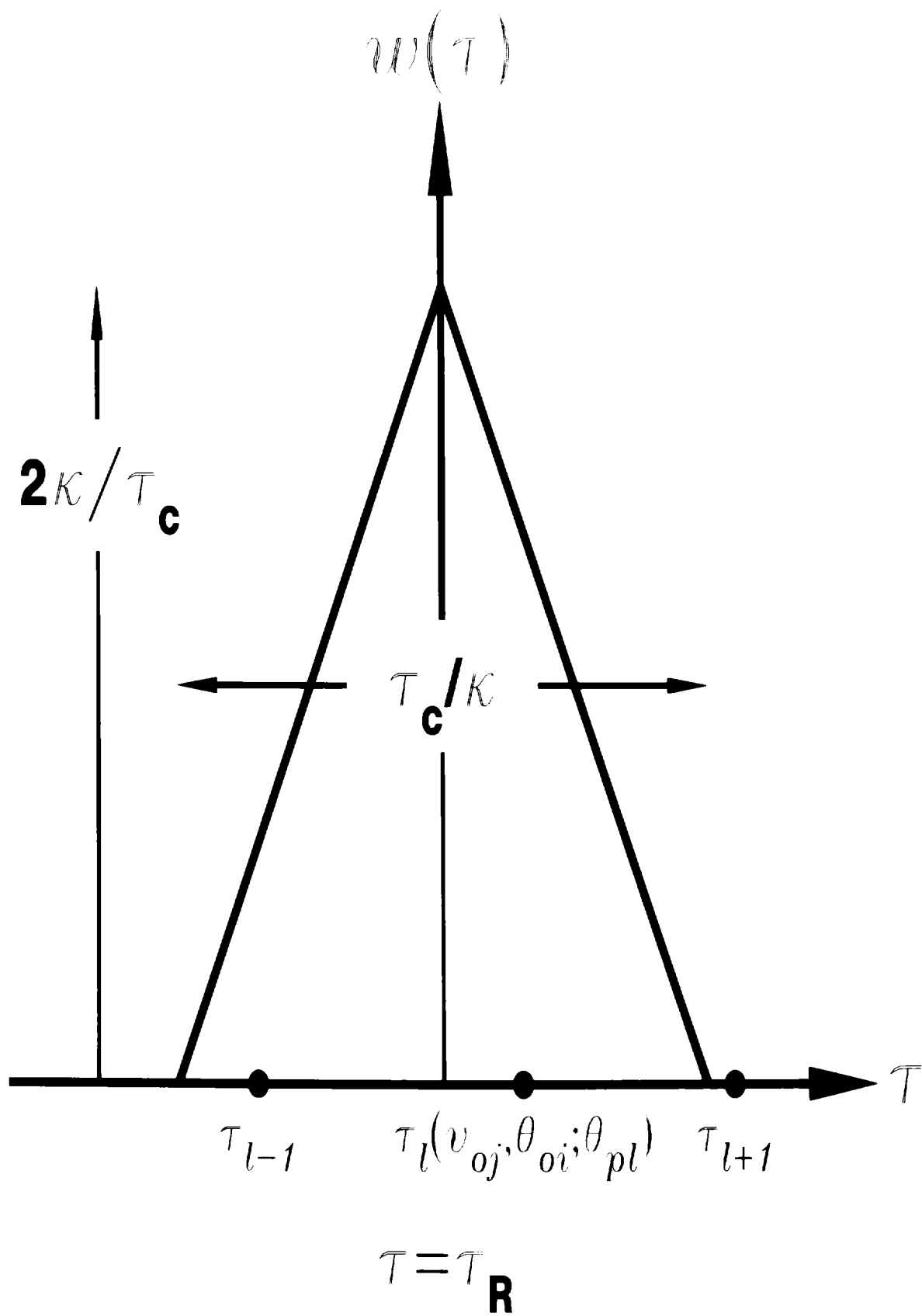


Figure 2

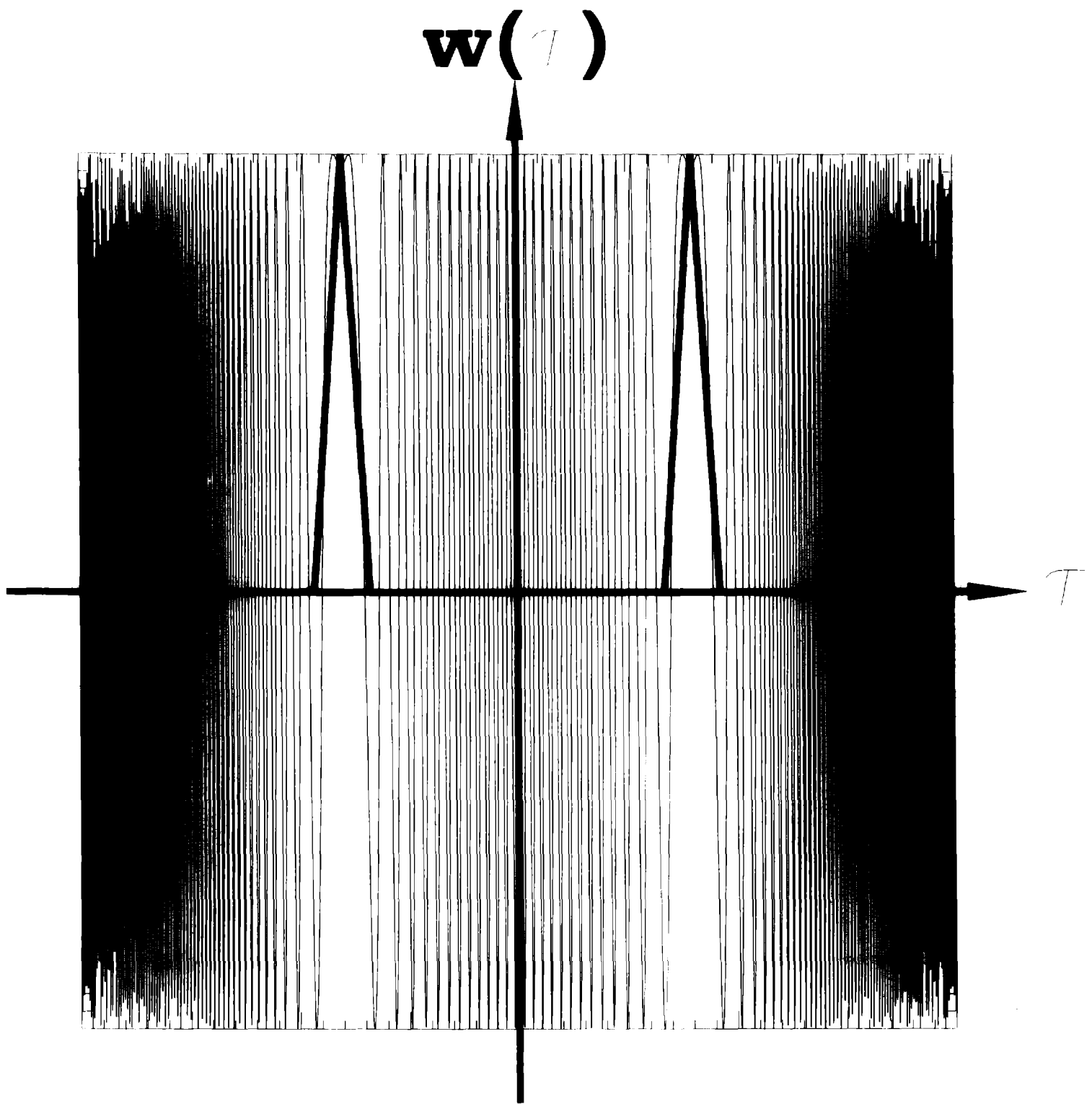


Figure 3a

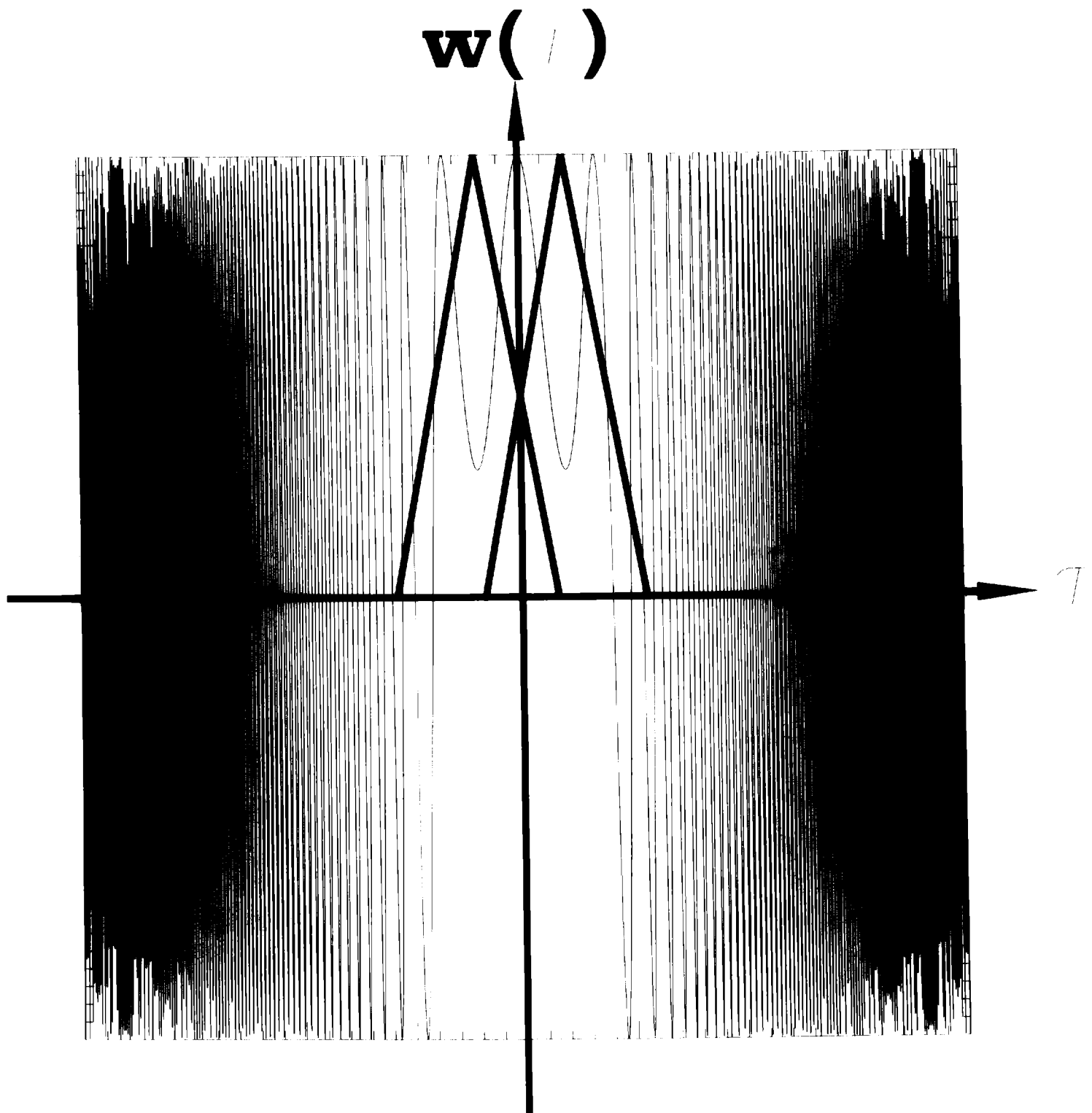


Figure 3b

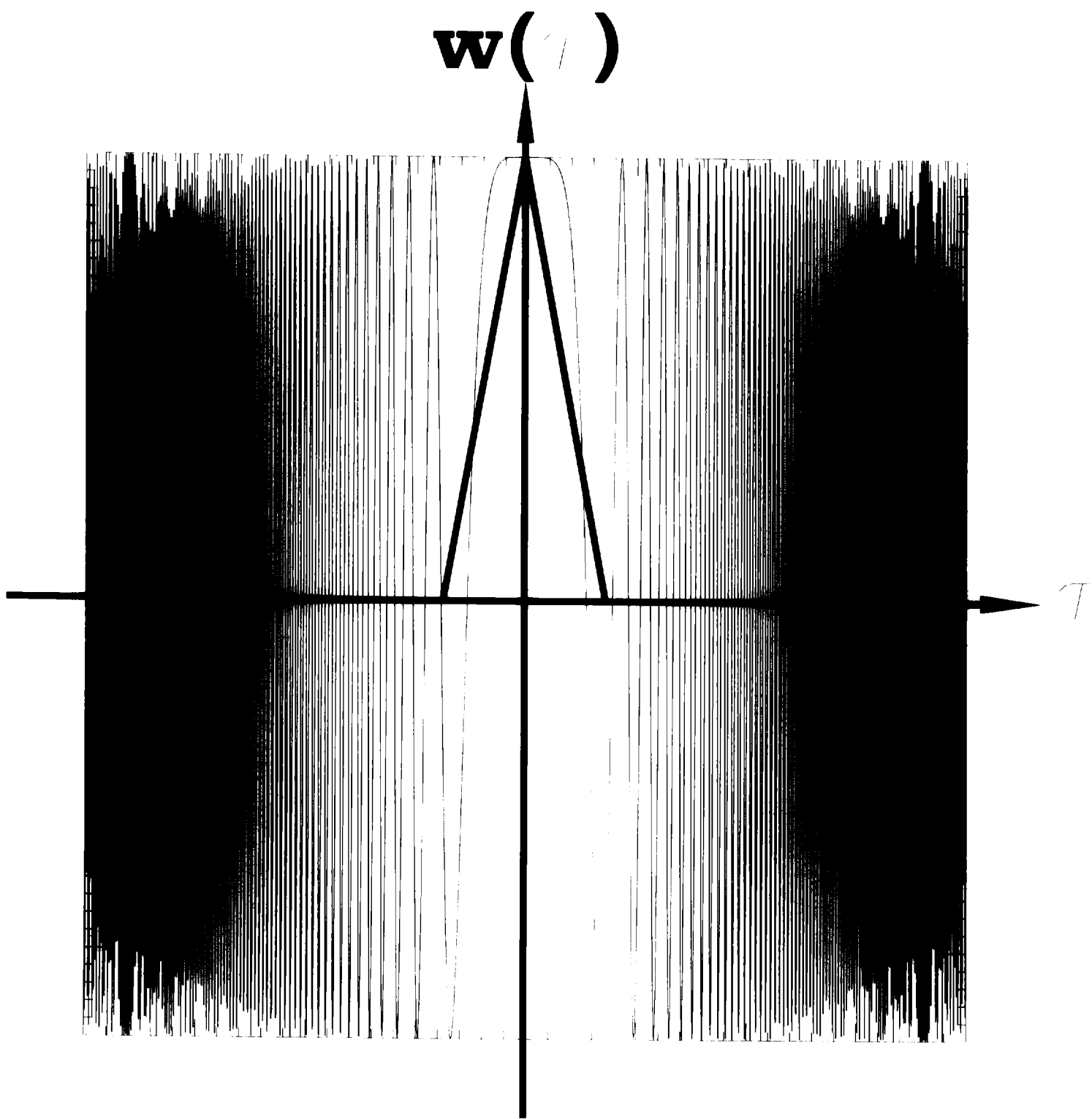


Figure 3c

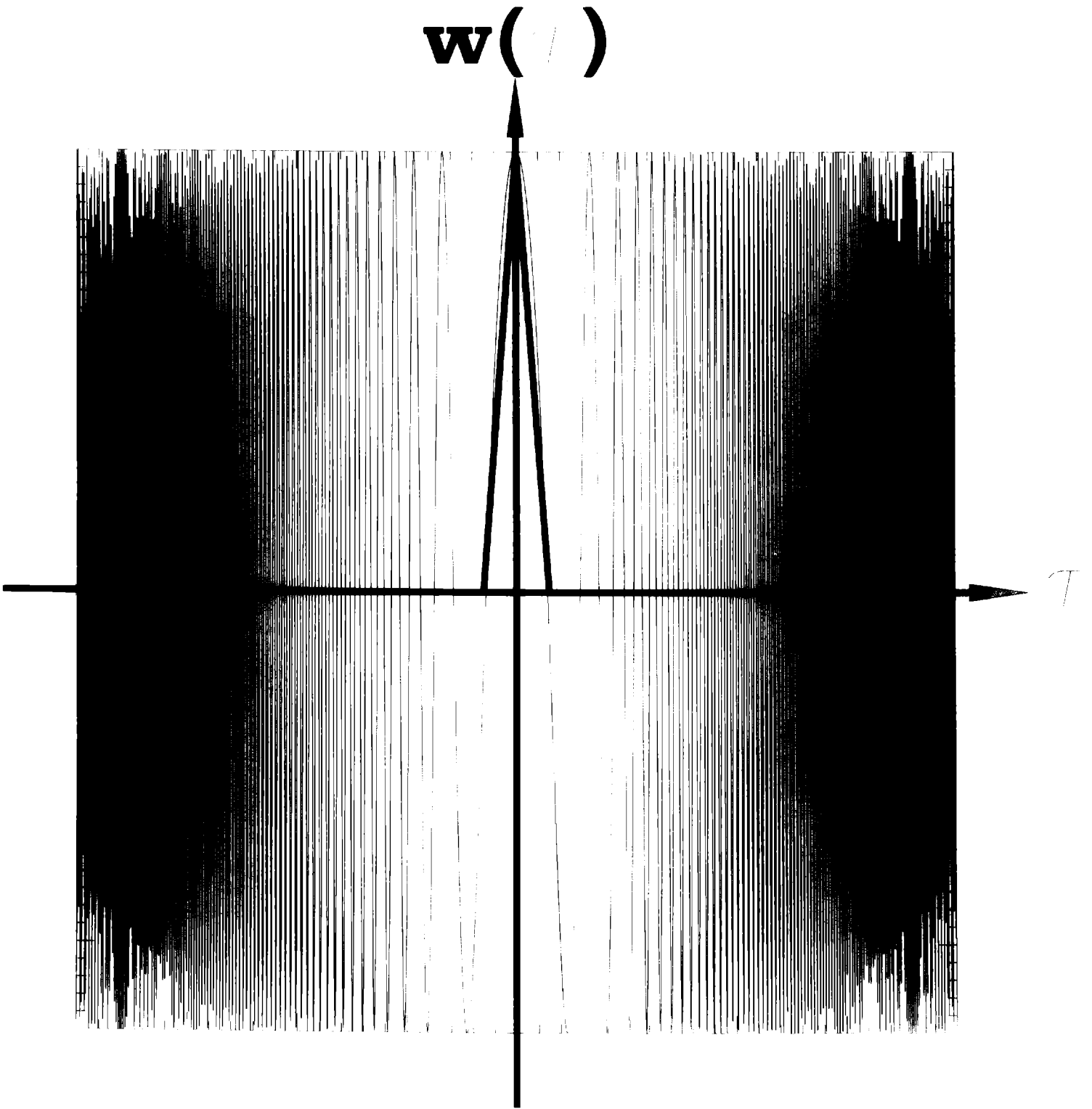


Figure 3d

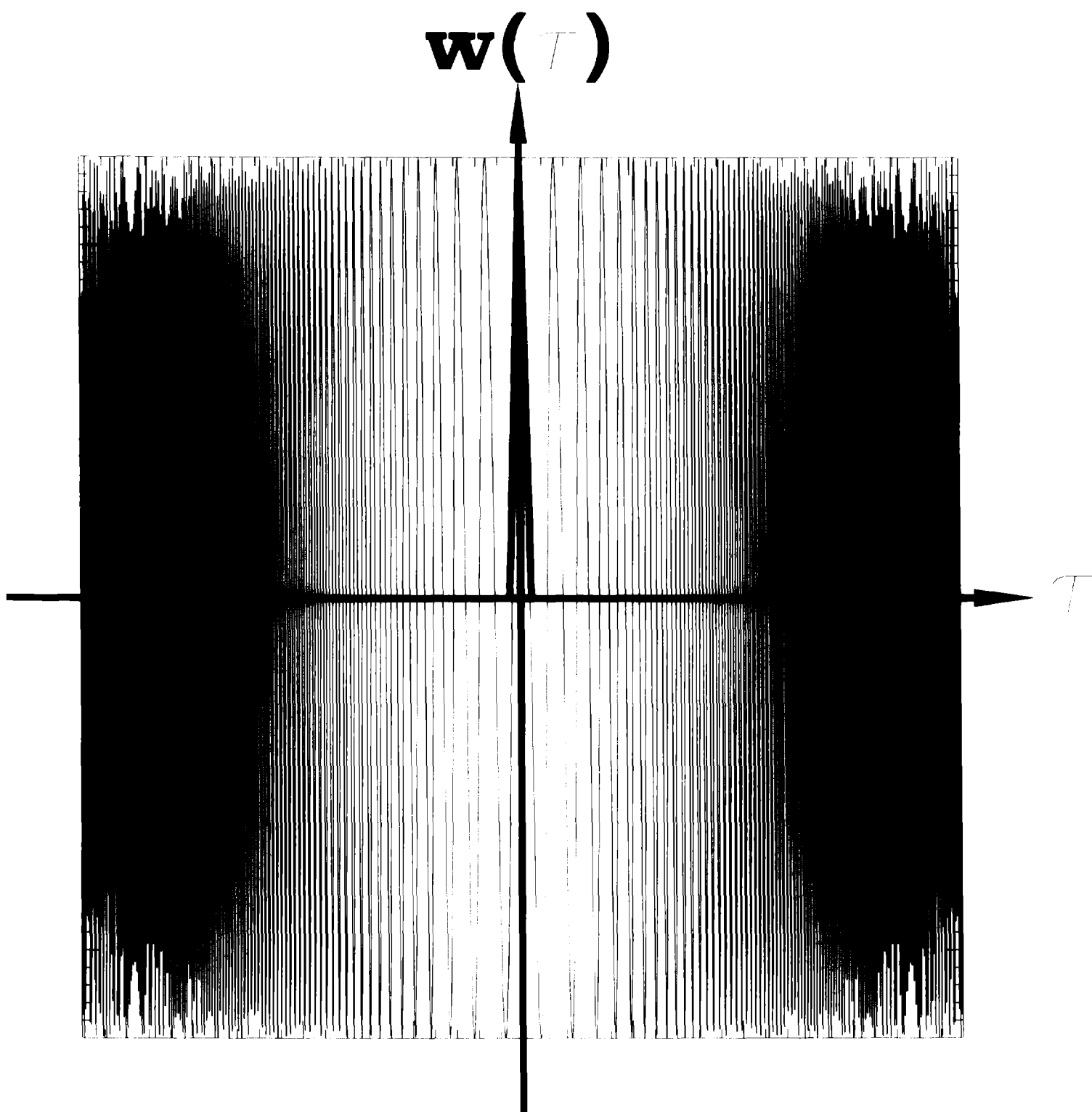
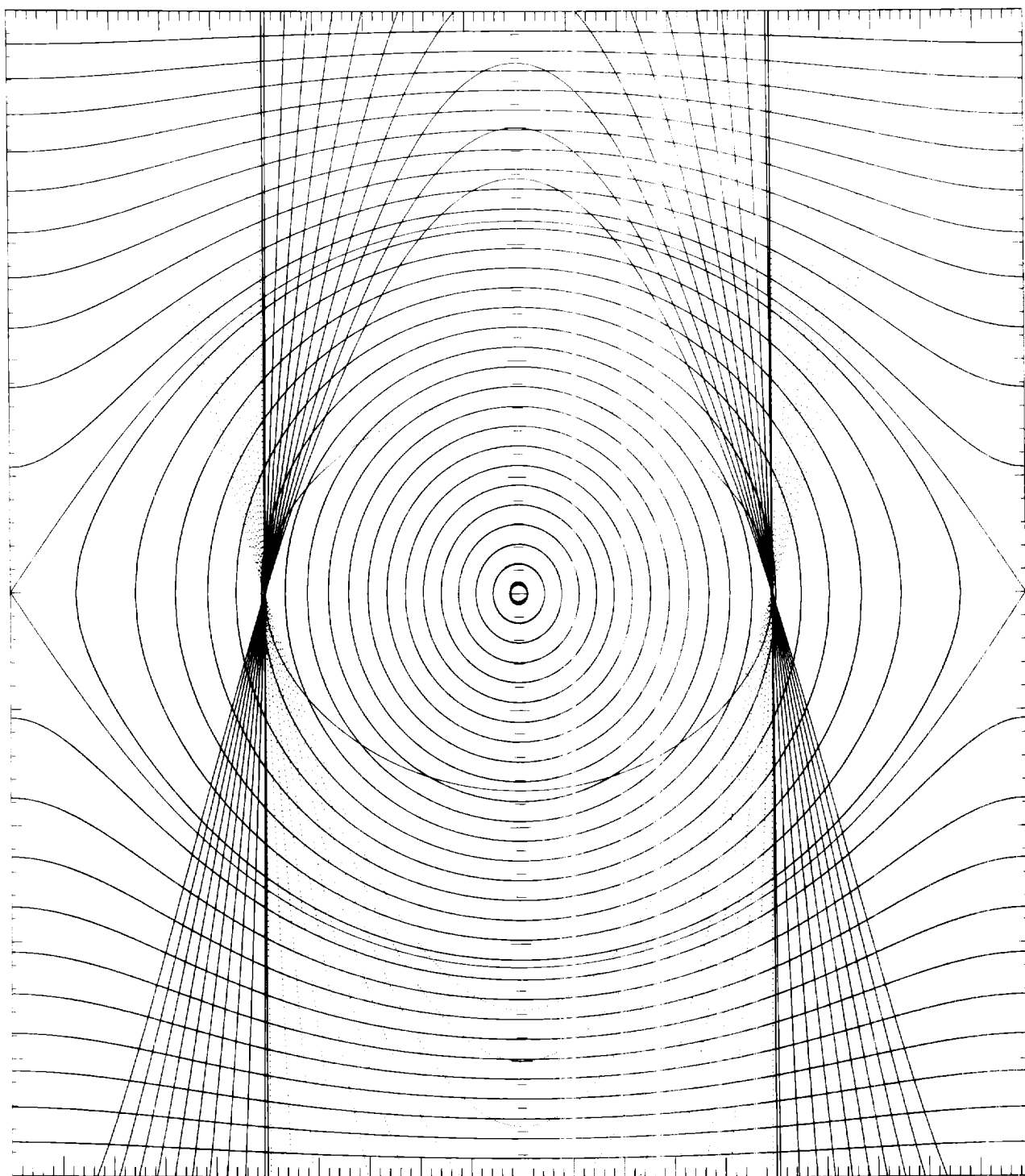


Figure 3e



$$\cos \theta \rightarrow p$$

Figure 4

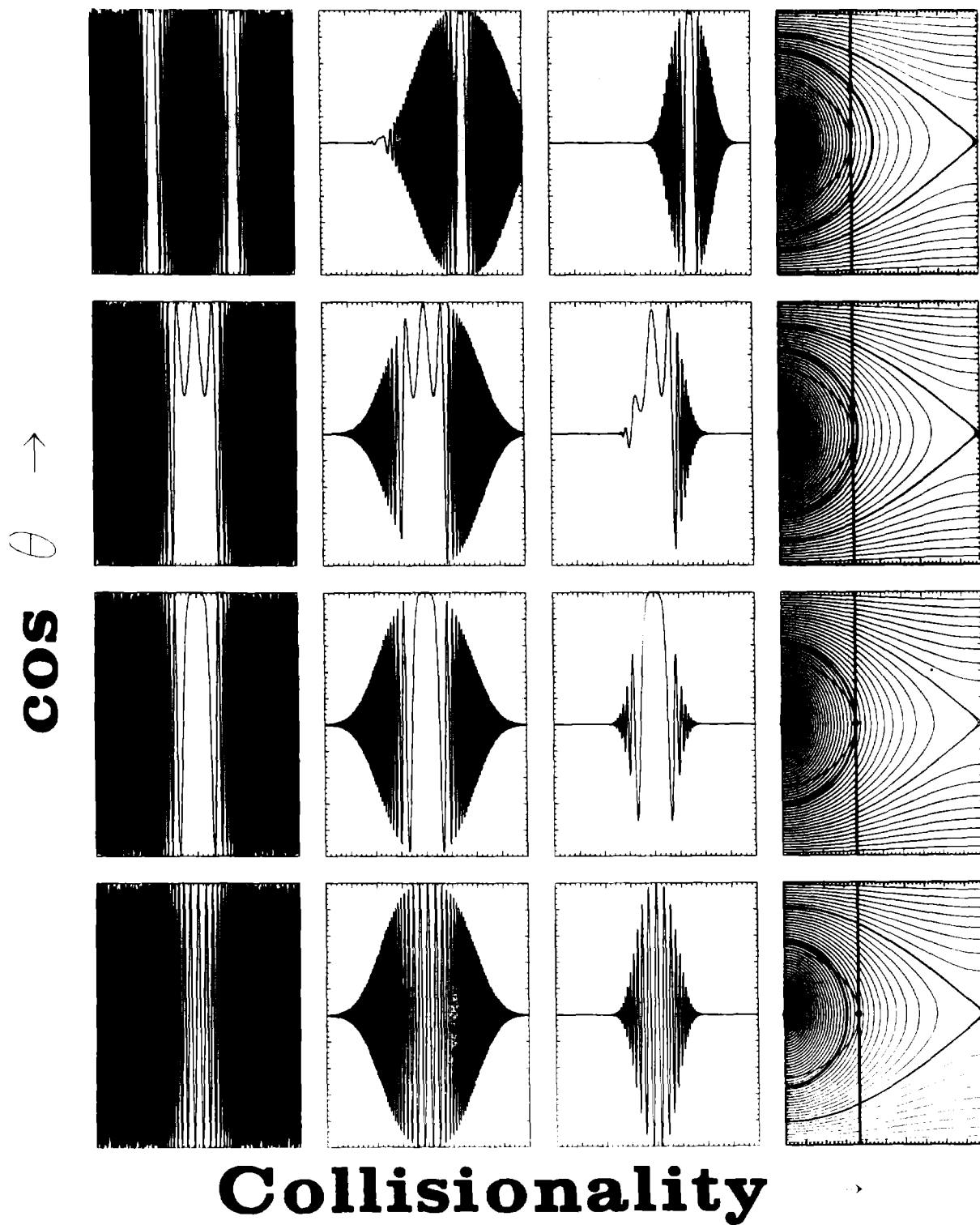
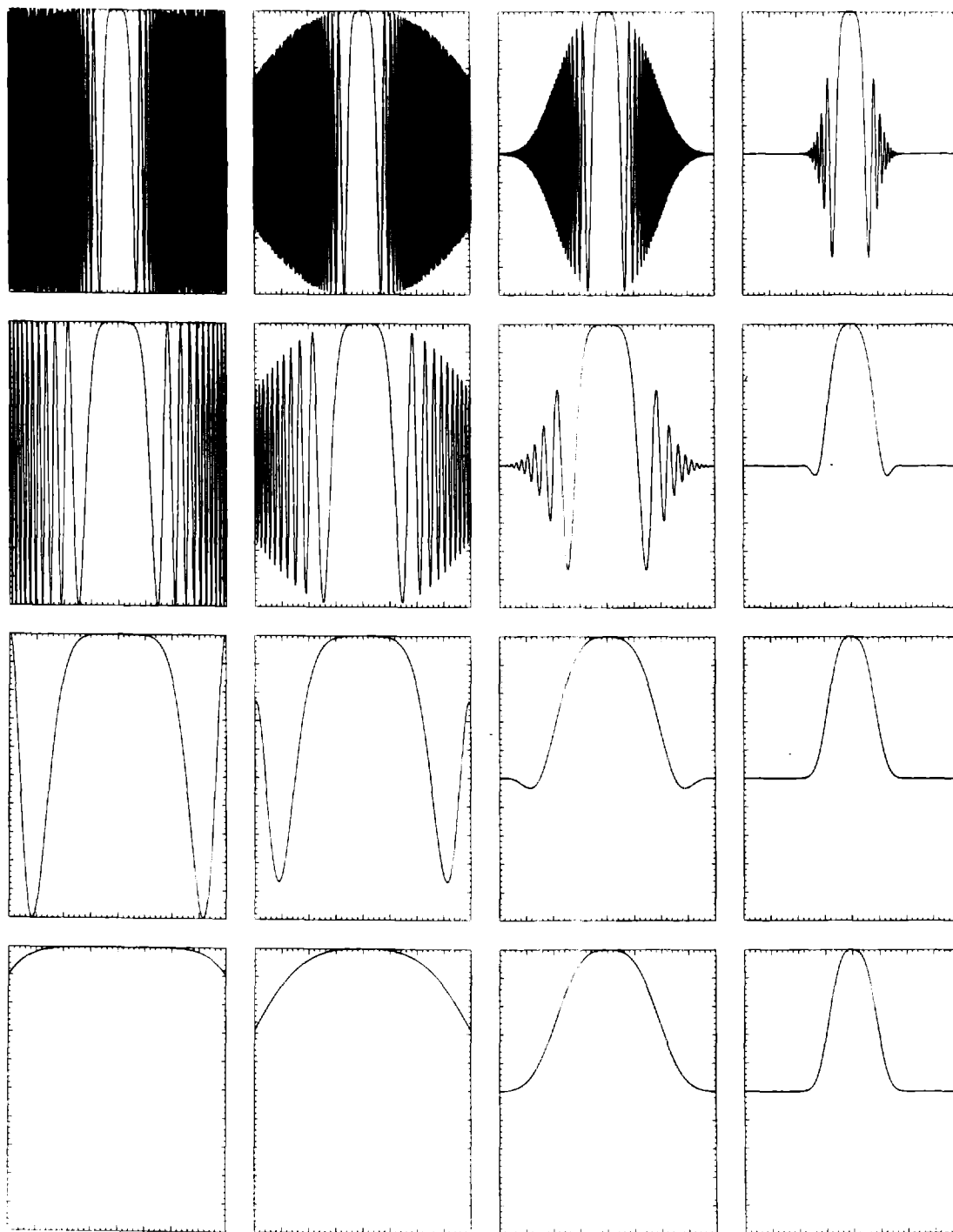


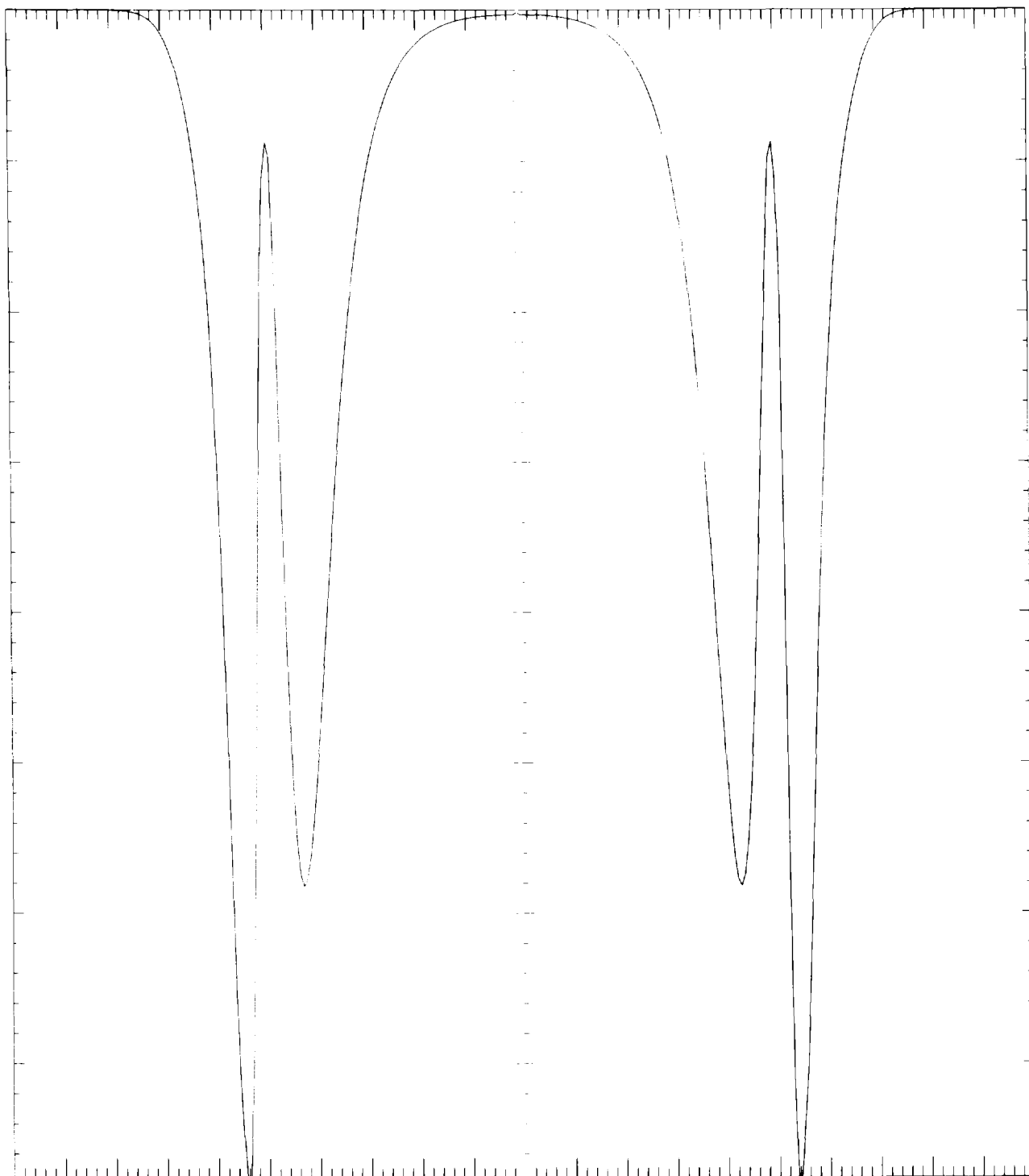
Figure 5

Magnetic Inhomogeneity →



Collisionality →

Figure 6



$$\cos \theta_p \rightarrow$$

Figure 7